

Nogueira, E. (2020). Thermal performance in heat exchangers by the irreversibility, effectiveness, and efficiency concepts using nanofluids. *Journal of Engineering Sciences*, Vol. 7(2), pp. F1–F7, doi: 10.21272/jes.2020.7(2).f1

Thermal Performance in Heat Exchangers by the Irreversibility, Effectiveness, and Efficiency Concepts Using Nanofluids

Nogueira E.

Department of Mechanics and Energy, State University of Rio de Janeiro, Brazil

Article info:

Paper received: April 28, 2020
 The final version of the paper received: August 14, 2020
 Paper accepted online: August 28, 2020

*Corresponding email:

elcionogueira@hotmail.com

Abstract. The objective of the work is to obtain the outlet temperatures of the fluids in a shell and tube heat exchanger. The second law of thermodynamics is applied through the concepts of efficiency, effectiveness, and irreversibility to analyze the results. Water flows in the shell, and a mixture of water-ethylene glycol is associated with fractions of nanoparticles flows in the tube. Water enters the shell at 27 °C, and the mixture comes to the tube at 90 °C. The mass flow is kept fixed in the shell, equal to 0.23 kg/s, and varies between 0.01 kg/s to 0.50 kg/s. Volume fractions equal to 0.01, 0.10, and 0.25 were considered for analysis, for both nanoparticles from Ag and Al₂O₃. Results for Reynolds number, heat transfer rate, efficiency, effectiveness, and irreversibility are presented for critique, discussion, and justification of the output data found. It is shown that the flow regime has a significant effect on the performance of the analyzed heat exchanger.

Keywords: thermodynamics, second law, ethylene glycol, volume fraction.

1 Introduction

The objective of the paper is to obtain the outlet temperatures in the shell and the tube heat exchanger, with nanofluid flowing in the tube (Ag or Al₂O₃) and a mixture of “water – ethylene glycol (EG 50 %)” flowing into the shell. The concepts of efficiency, effectiveness, and irreversibility were applied to the system to achieve the objective of analyzing and discuss the results.

According to A. Fakheri [1], the concept of efficiency leads to a new form of analysis for heat exchangers. The concept of efficiency is defined as the ratio of the current heat exchange of the heat exchanger to that transferred by an ideal heat exchanger. The ideal heat exchanger transfers the maximum amount of heat, and generates the minimum

expressions of efficiency are similar to the efficiency of a constant area fin with an insulated tip.

If the entropy in the compound elements is minimized, the reduction of irreversibility also occurs in the system. A. Bejan [2] presents a comprehensive review of the literature, where the focus lies on the fundamental mechanisms responsible for the generation of entropy in the form of heat and the viscous dissipation generated by the flow. The article provides a comprehensive review of analyzes based on the second law of thermodynamics related to heat and mass transfer.

2 Literature Review

M. Molana [3], in his review of the literature it confirms the increase in the number of Nusselt with the use of nanofluids in the heat exchangers an increase in the pumping power. The maximum observed increase in heat transfer is 325 % in shell and tube heat exchangers, and this maximum heat transfer enhancement occurs at the highest nanofluid volume concentration, in most cases.

Air bubble injection inside shell and tube increases heat exchanger by creating turbulence, and the heat transfer characteristic is enhanced with the insertion of nanoparticles volumetric concentration. Experiments have shown that the heat transfer rate increases by 23–38 % to the tube containing nanoparticles Gaurav Thakur and G. Singh [4].

A seawater source heat pump is used as the cold and heat source to provide a ship with the necessary reducing the consumption of energy. A theoretical model was established based on heat exchanger efficacy and efficiency. The exergy transfer was evaluated with graphene nanoparticles and with different concentrations. The effectiveness demonstrates the benefit of using graphene in concentrations in weight of 0.01–0.10 %, as they are more efficient in transferring exergy than those

with levels of 0.5–1.0 %. When the graphene nanofluid concentration is remarkably high, the resistance caused by the increase in viscosity causes a decrease in efficiency Z. Wang et al. [5].

K. Y. Leong et al. [6] confirmed that shell and tube heat exchangers with the addition of nanofluids provide excellent thermal performance; however, the viscous dissipation increases with the addition of nanoparticles. Another major factor for the thermal performance of shell and tube exchangers is related to the number and arrangement of the deflectors. They present a study that focuses on the analysis of the influence of segmental deflectors on shell and tube heat exchangers. The results indicate that 50° helical deflectors have less entropy generation.

Distilled water with TiO₂ nanoparticles was used as a test liquid using three different volume concentrations (0.1, 0.2, and 0.35 %) by M. P. S. Bharadwaj and S. S. Babu [7]. They insert three-wire coil of the uniform pitch to create a continuous impinging swirl flow along the tube wall in a 2S-2T (two shell passes – two tube passes). There is a significant improvement in the Nusselt number (from 13.5 to 21.3 %) for the Reynolds number between 3000 and 8000 in the nanofluid.

J. E. Igwe and C. S. Agu [8] evaluated the performance of various proportions of ethylene glycol and silicon carbide, using a shell and tube heat exchanger in a counterflow arrangement, and 57 % was the higher efficiency of the system using water-sic as the base fluid for cooling.

S. Almurtaji et al. [9] provides a systematic review of the state-of-the-art heat exchanger technology with the primary purpose of to emphasize the importance of how nanofluids can increase the thermal efficiency for future applications. They emphasize that a small number of papers reported that there is an optimum solid concentration at which the thermal-hydraulic performance reaches a maximum level and that the effects of the sedimentation and corrosion by nanofluids need to be explored.

Yue Sun et al. [10] present an article where a numerical simulation is conducted to investigate a shell and tube heat exchanger with inclined trefoil-hole baffles (STHX-IT) and segmental baffles (STHX-SG). The STHX-IT has a superior performance because of the lower heat transfer rate with a more significant reduction in the pressure drop than conventional STHX-SG. It can be concluded that the new STHX-IT is effective in enhancing the overall performance of the shell side and provides a solution to replace the STHX-SG.

S. S. Krishnan et al. [11] studied the heat transfer characteristics of Shell and the tube and other heat

exchangers, using miscible and immiscible systems. The experiment evaluated the effect of variations in the flow of cold and hot fluids in a shell and tube heat exchanger. They concluded that the results from the tests could help to optimize the shell and tube heat exchanger since a maximum efficiency at minimal costs will have an enormous impact in the industrial world.

The performance of the shell and tube heat exchanger was studied by A. A. H. Mostafa, E. E. Khalil and G. El-Hariry [12] varying the parameters and using CFD software. The results demonstrated sensitivity to the model of turbulence. They showed that the heat exchanger baffles were optimized to give the maximum shell side Nusselt number, and this conclusion is a benefit to energy conservation.

J. Alobar, S. Tayal, and M. Alasadi [13] reported an experimental study of a nanofluid with volume concentrations of Al₂O₃ nanofluid 0.3–2.0 % flowing in a shell and tube heat exchanger under turbulent flow conditions. The heat transfer coefficient increases with the increase in mass flow rate and with the increase in the volumetric concentration of Al₂O₃.

3 Research Methodology

Primary data: One pass in the tube, one pass in the shell, and three baffles. Number of tubes $N_T=32$; $L_S=0.762$ m; $d_S=0.508$ m; $d_T=0.0127$ m; $T_{c_i}=27$ °C; $T_{h_i}=90$ °C.

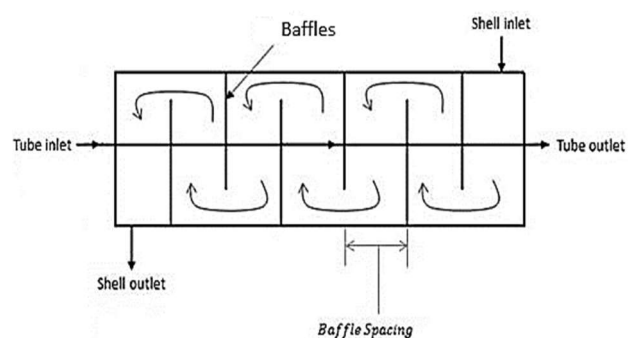


Figure 1 – Schematic representation of the shell and tube heat exchangers in countercurrent flow

The flow in the shell is fixed equal to 0.23 kg/s. Flow rates in the tube vary from 0.0 kg/s to 0.5 kg/s, and fractions in volume equal to 0.01, 0.10, and 0.25 were considered for analysis, for both nanoparticles. Fluid enters the tube at 90 °C, and the shell at 27 °C.

Properties of the fluids and nanoparticles are summarized in Table 1.

Table 1 – Properties of the fluids and nanoparticles

Parameter	Shell cold fluid	Tube hot fluid	Ag	Al ₂ O ₃	EG 50 %
k , W/(m·K)	0.60	0.67	429	31.9	0.422
C_p , J/(kg·K)	4180	4216	235	873	3879
μ , 10 ⁻³ kg/(m·s)	0.758	0.303	–	–	0.528
ρ , kg/m ³	997	970	10,500	3,950	1,058
ν , 10 ⁻⁶ m ² /s	0.800	0.334	–	–	0.499
α , 10 ⁻⁶ m ² /s	0.143	0.168	174	110	0.103
Pr	5.59	1.99	–	–	3.87

If the volume fraction (V_{EG}) of ethylene glycol is provided, the properties of the base fluid can be obtained through the equations below:

$$\mu_{solution} = \mu_{EG} V_{EG} + (1 - V_{EG})\mu_{wh}; \quad (1)$$

$$\mu_{solution} = \mu_{EG} V_{EG} + (1 - V_{EG})\mu_{wh}; \quad (2)$$

$$\rho_{solution} = \rho_{EG} V_{EG} + (1 - V_{EG})\rho_{wh}; \quad (3)$$

$$k_{solution} = k_{EG} V_{EG} + (1 - V_{EG})k_{wh}; \quad (4)$$

$$Cp_{solution} = Cp_{EG} V_{EG} + (1 - V_{EG})Cp_{wh}. \quad (5)$$

The properties of the nanofluid, for volume fraction (ϕ) of the Copper Oxide (CuO), is given by the following equations:

$$\rho_h = \phi \rho_{particle} + (1 - \phi)\rho_{solution}; \quad (6)$$

$$\mu_h = \mu_{solution}(1 - 0.19\phi + 306\phi^2); \quad (7)$$

$$Cp_h = [\phi \rho_{particle} Cp_{particle} + (1 - \phi)\rho_{solution} Cp_{solution}] / \rho_c; \quad (8)$$

$$k_h = [(k_{particle} + 2k_{solution} + 2(k_{particle} - k_{solution})(1 - 0.1)^3\phi) / [k_{particle} + 2k_{solution}(k_{particle} - k_{solution}) \cdot (1 + 0.1)^2\phi]] k_{solution}. \quad (9)$$

The heat exchange area is obtained by:

$$A_h = \pi d_T L_s N_T. \quad (10)$$

The Nusselt number in the tube is equal to

$$Nu_h = 4.364 + 0.0722 Re_h Pr_h \frac{d_T}{L_s}$$

for

$$Re_h < 2100 \quad (11)$$

or calculated as follows:

$$Nu_h = 0.023 Re_h^{0.8} Pr_h^{0.4}, \quad (12)$$

where the Reynolds number in the tube

$$Re_h = 4\dot{m}_h / (N_T \pi d_T \mu_h). \quad (13)$$

Then the convective heat transfer coefficient in the tube is given by:

$$h_h = \frac{Nu_h k_h}{d_T}. \quad (14)$$

The Reynolds number in the shell is equal to

$$Re_c = \frac{4\dot{m}_c}{\pi d_e \mu_c}; \quad (15)$$

$$Nu_c = 4.364 + 0.0722 Re_c Pr_c \frac{d_e}{L_s}$$

$$\text{for } Re_c < 2100 \quad (16)$$

or

$$Nu_c = 0.023 Re_c^{0.8} Pr_c^{0.3} \quad (17)$$

are the Nusselt number in the shell.

The shell equivalent diameter:

$$d_e = \frac{1.27}{d_T} (P_T^2 - 0.785 d_T^2). \quad (18)$$

The convection heat transfer coefficient in the shell

$$h_c = \frac{Nu_c K_c}{d_e}, \quad (19)$$

and

$$P_T = 1.25 d_T \quad (20)$$

is the tube pitch, for square cross-section.

Additionally,

$$D_B = d_s \left(\frac{N_T}{0.125} \right)^{\frac{1}{2.207}} \quad (21)$$

$$BS = 0.4 D_B, \quad (22)$$

where D_B and B_S are the bundle diameter and baffles space, respectively.

The number of baffles:

$$B_B = \frac{L_s}{B_S} \quad (23)$$

The overall convection heat transfer coefficient:

$$U_o = \frac{1}{\frac{1}{h_h} + \frac{1}{h_c}}. \quad (24)$$

The thermal capacities of both fluids are given by:

$$C_c = \dot{m}_c Cp_c \text{ and } C_h = \dot{m}_h Cp_h; \quad (25)$$

$$NTU = \frac{A_h U_o}{C_{min}} \quad (26)$$

where NTU is the Number of Thermal Units, and C_{min} is the lowest value among thermal capacities.

The effectiveness of the shell and tube heat exchanger [1]:

$$\varepsilon = \frac{1}{\frac{1}{\eta NTU} + \frac{(1 + C^*)}{2}} \quad (27)$$

The efficiency of the heat exchanger [1]:

$$\eta = \frac{Tanh(F_a)}{F_a} \quad (28)$$

where

$$F_a = \frac{NTU(1 - C^*)}{2} \quad (29)$$

and

$$C^* = \frac{C_{max}}{C_{min}} \quad (30)$$

$$Q_{Actual} = \frac{(Th_i - Tc_i)C_{min}}{\frac{1}{\eta NTU} + \frac{(1 + C^*)}{2}} \quad (31)$$

Q_{Actual} is the heat transfer rate, depending on the efficiency and temperature of the fluids [1], and

$$Q_{max} = C_{min}(Th_i - Tc_i) \quad (32)$$

is the maximum heat transfer rate.

Additionally,

$$Th_o = Th_i - \frac{Q_{Actual}}{\dot{m}_h C_p h} \quad (33)$$

and

$$Tc_o = Tc_i + \frac{Q_{Actual}}{\dot{m}_c C_p c} \quad (34)$$

are the outlet temperatures, and

$$\sigma_T = \frac{C_h}{C_{min}} \ln\left(\frac{Th_o}{Th_i}\right) + \frac{C_c}{C_{min}} \ln\left(\frac{Tc_o}{Tc_i}\right) \quad (35)$$

is the thermal irreversibility [2].

4 Results and discussion

Figure 2 shows the results for the number of Reynolds, with the concentration of the nanoparticles as a parameter. It can be seen that the number of Reynolds is smaller for a higher fraction in volume for the same mass flow rate of the nanofluid. This result has a significant influence on the thermal performance of a heat exchanger, as already discussed by E. Nogueira [14]. The viscosity of the nanofluid increases with the addition of the volumetric

fraction of the nanofluid. The type of nanoparticle has not to influence in the Reynolds number, in this case.

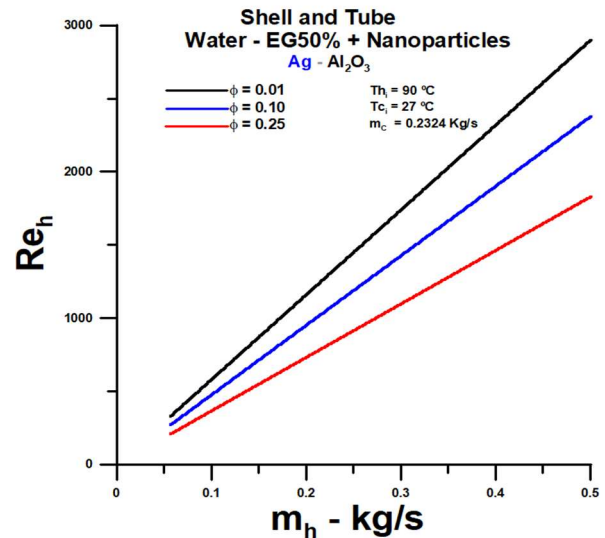


Figure 2 – Reynolds number vs. mass flow rate

The heat transfer rate is higher when the volume fractions are higher, as can be seen from Figure 3 below. There is no significant difference between heat transfer rates when considering silver nanoparticles (Ag) and aluminum oxide (Al_2O_3), with a slight advantage for silver nanoparticles. When the flow changes from laminar regime to turbulent regime, there is an abrupt drop in the heat transfer rate, with a lower rate of heat transfer in turbulent regime, within the analyzed flow range. For a fraction of volume equal to 0.01, the heat transfer rates are practically identical, in qualitative terms. Due to the flow laminarization effect, the results presented are, to a greater extent, within the laminar regime range. When the laminar regime occurs, the impact of higher diffusivity is predominant compared to the effect of internal convection. It can be observed, in highlight, that the rate of heat transfer significantly approaches the maximum rate of heat transfer for low values of the Reynolds number.

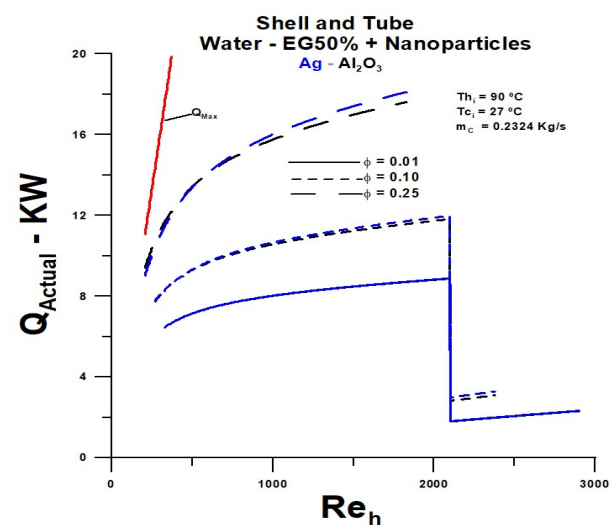


Figure 3 – Heat transfer rate vs. Reynolds number

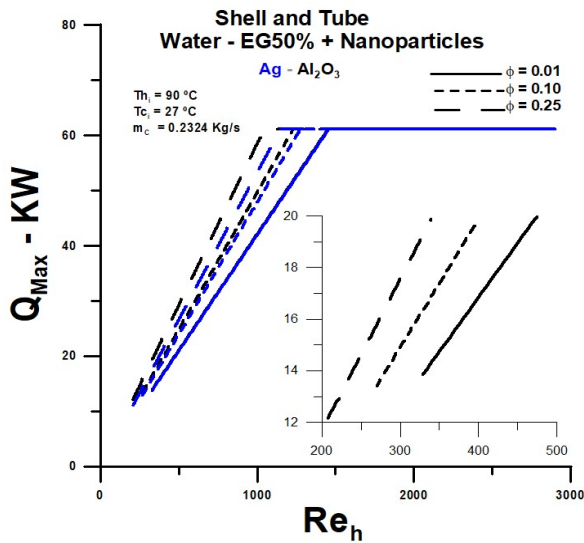


Figure 4 – Maximum heat transfer rate vs. Reynolds number

For smaller volume fractions of the nanoparticles, the heat transfer rate is much lower than the maximum, as shown in the results presented in Figures 3 and 4. The heat transfer is below 12 kW and the maximum above 14 kW, as can be seen in the highlight of Figure 4. This aspect has high relevance concerning the outlet temperatures of cold and hot fluids, irreversibility, effectiveness, and thermal efficiency.

The outlet temperatures of the cold fluid, Figure 5, are identical in qualitative terms to the heat transfer rate. The highest temperatures occur precisely where the heat transfer rate is maximum and maintain the proportionality to the results presented in Figure 4.

The results for the hot fluid outlet temperature are shown in Figure 6. The lowest temperature values occur for the most considerable fraction in the volume of the nanoparticles, where the heat transfer rate approaches the maximum. For smaller fractions, the outlet temperatures are higher, and there is no significant difference between them. Silver performs better at higher flow rates within the range of the analyzed Reynolds numbers. For lower mass flow rates, performances are similar.

The thermal performance is superior, as demonstrated by the results of temperature profiles and heat transfer rate, the effectiveness is maximum, and the irreversibility is high, as shown in Figures 7 and 8. For smaller volume fractions of the nanoparticles to irreversibility and effectiveness drop significantly, as can be seen in the highlights. However, the effect of greater thermal irreversibility, for laminar flow in the tube, affects and is more relevant to effectiveness.

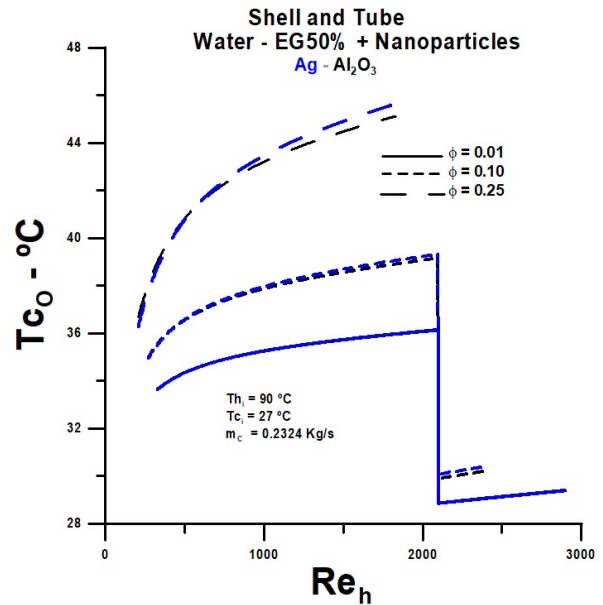


Figure 5 – Cold fluid outlet temperature

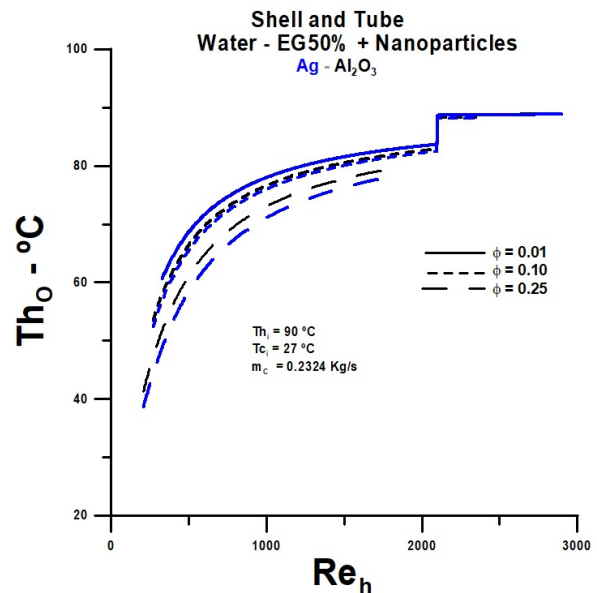


Figure 6 – Hot fluid outlet temperature

Results opposite to those already observed occur about thermal efficiency, Figure 9. For smaller volume fractions of the nanoparticles, the efficiency is maximum in almost all the flow range analysis.

Irreversibility and effectiveness are high, efficiency is low, with emphasis on the efficiency of copper oxide, which presents very low values for lower flow rates and a point of maximum efficiency for Reynolds number close to 800, when the volume fraction is the tallest.

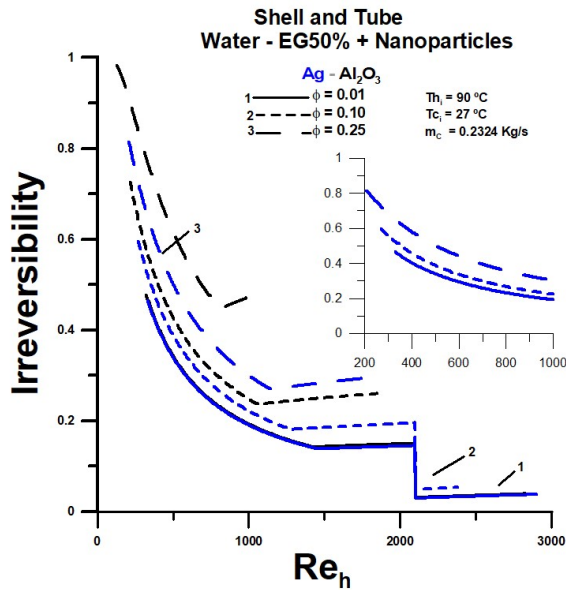


Figure 7 – Irreversibility versus Reynolds number

Efficiency, within the context in question, does not have a significant connection with the outlet temperature profiles. Where efficiency is high, the results are not favorable.

The higher thermal dissipation, associated with the greater irreversibility, has greater relevance for the temperature profiles and the effectiveness where the flow regime is laminar. Also, the influence of the laminar regime is pronounced for lower values of the Reynolds number, where the conductive effect of heat transfer is more relevant, and the thermal dissipation is more pronounced. At low flow rates of nanofluid in the tube, and a high fraction in the volume of nanoparticle, the thermal performance is not efficient, but it is effective.

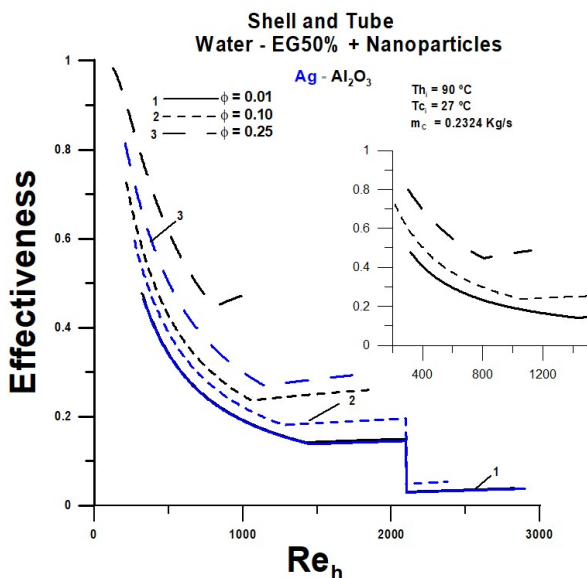


Figure 8 – Effectiveness versus Reynolds number

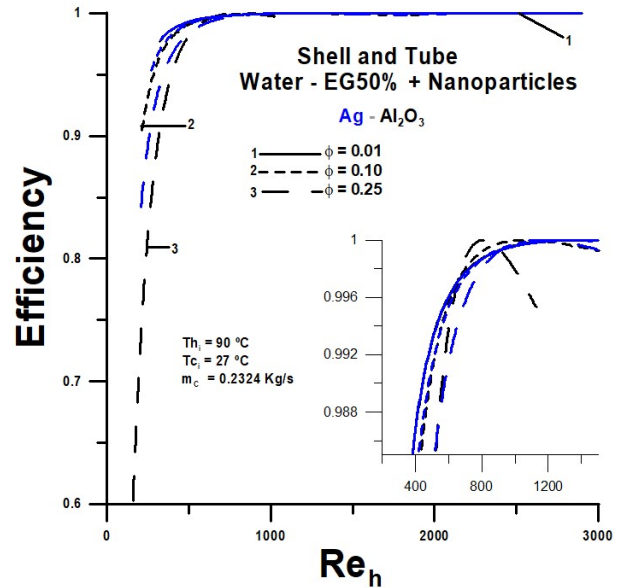


Figure 9 – Efficiency versus Reynolds number

The heat transfer rate approaches the maximum heat transfer rate when the effectiveness and irreversibility present high values, for Reynolds numbers below 500. In contrast, the outlet temperatures of the fluid in the tube present the lowest values, with values slightly smaller for silver.

There were no variations in the flow rate in the shell, but it should be noted that the flow is turbulent, $Re_c = 3.1 \cdot 10^4$, and the heat transfer coefficient is relatively high: $h_c = 7.37 \text{ kW}/(\text{m}^2 \text{ K})$. These values can affect heat transfer and have a positive influence on the values of the overall heat convection coefficient.

5 Conclusions

High effectiveness, associated with high irreversibility, is the parameter that leads to lower temperatures in the tube when the Reynolds number is relatively small in a laminar regime. Indeed, heat transfer rates that approach the maximum possible within the range under analysis are desirable.

Efficiency is high in almost all the situations analyzed in this study. However, for fractions in a volume equal to 0.25, efficiency has a significant drop, and silver, which has greater thermal diffusivity than aluminum oxide, has higher efficiency and lower outlet temperature for the fluid in the tube. It is to be expected that a higher fraction in the volume of nanoparticle has associated greater viscous dissipation, as reported in the literature.

In a laminar regime, the conductive effect is relevant concerning heat transfer, and high-volume fractions of nanoparticles have a more considerable influence to obtain lower outlet temperatures of the nanofluid in the tube. In this case, a higher value for thermal conductivity enables greater thermal efficiency.

References

1. Fakhri, A. (2007). Heat exchanger efficiency. *Transactions of the ASME*, Vol. 129, pp. 1268–1276.
2. Bejan, A. (1987). The thermodynamic design of heat and mass transfer processes and devices. *Heat and Fluid Flow*, Vol. 8(4), pp. 258–276.
3. Molana, M. (2016). A comprehensive review on the nanofluids application in the tubular heat exchangers. *American Journal of Heat and Mass Transfer*, Vol. 3(5), pp. 352–381.
4. Thakur, G., Singh, G. (2017). An experimental investigation of heat transfer characteristics of water-based Al₂O₃ nanofluid operated shell and tube heat exchanger with air bubble injection technique. *International Journal of Engineering and Technology*, Vol. 6(4), pp. 83–90.
5. Wang, Z., Han, F., Ji, Y., Li, W. (2020). Performance and exergy transfer analysis of heat exchangers with graphene nanofluids in seawater source marine heat pump system. *Energies*, Vol. 13, 1762, doi: 10.3390/en13071762.
6. Leong, K. Y., Saidur, R., Khairulmaini, M., Michael, Z., Kamyar, A. (2012). Heat transfer and entropy analysis of three different types of heat exchangers operated with nanofluids. *International Communications in Heat and Mass Transfer*, Vol. 39, pp. 838–843.
7. Bharadwaj, M. P. S., Babu, S. S. (2017). Heat transfer enhancement in 2S-2T shell and tube heat exchanger with wire coil and twisted tape turbulators using TiO₂ nanofluid. *International Journal of Mechanical Engineering and Technology*, Vol. 8(7), pp. 846–859.
8. Igwe, J. E., Agu, C. S. (2016). Comparative analysis of different fluids in one shell pass and two tube heat exchanger. *American Journal of Engineering Research*, Vol. 5(8), pp-81–87.
9. Almurtaji, S., Ali, N., Teixeira, J. A., Addali, A. (2020). On the Role of nanofluids in thermal-hydraulic performance of heat exchangers – a review. *Nanomaterials*, Vol. 10, 734, doi: 10.3390/nano10040734.
10. Sun, Y., Wang, X., Long, R., Yuan, F., Yang, K. (2019). Numerical investigation and optimization on shell side performance of a shell and tube heat exchanger with inclined trefoil-hole baffles. *Energies*, Vol. 12, 4138, doi: 10.3390/en12214138.
11. Krishnan, S. S., Archana, S. P., Dayanidhi, R. S., Jayashruthi, R. (2019). Experimental and Investigation of shell and tube heat exchanger. *International Journal of Engineering and Techniques*, Vol. 5(4), pp. 1–5.
12. Mostafa, A. A. H., Khalil, E. E., El-Hariry, G., Abdelmaksoud, W. A., Saad, E. M. (2017). Shell and tube heat exchanger performance. *AIAA Propulsion and Energy Forum of the 15th International Energy Conversion Engineering Conference*, pp. 1–13.
13. Albadr, J., Tayal, S., Alasadi, M. (2013). Heat transfer through heat exchanger using Al₂O₃ nanofluid at different concentrations. *Case Studies in Thermal Engineering*, Vol. 1, pp. 38–44.
14. Nogueira, E. (2020). Thermal-hydraulic performance of graphene nanoribbon and silicon carbide nanoparticles in the multi-louvered radiator for cooling diesel engine. *Journal of Engineering Sciences*, Vol. 7(1), pp. F22–F29, doi: 10.21272/jes.2020.7(1).f2.